The Canadian Mineralogist
Vol. 35, pp. 887-897 (1997)

RUTHENIAN PYRITE AND NICKELOAN MALANITE FROM THE IMANDRA LAYERED COMPLEX, NORTHWESTERN RUSSIA

ANDREI Y. BARKOV[1]

Institute of Geosciences and Astronomy, University of Oulu, FIN-90570 Oulu, Finland

TAPIO A.A. HALKOAHO

Department of Geology, University of Turku, FIN-20014 Turku, Finland

KAUKO V.O. LAAJOKI AND TUOMO T. ALAPIETI

Institute of Geosciences and Astronomy, University of Oulu, FIN-90570 Oulu, Finland

RAIJA A. PEURA

Institute of Electron Optics, University of Oulu, FIN-90570 Oulu, Finland

Abstract

Ruthenian pyrite and an unusual, Ir–Rh-poor nickeloan malanite occur in a chromitite layer in the Lower Zone of the Early Proterozoic Imandra layered complex, northwestern Russia. A very low amount of the base-metal sulfide minerals, *BMS* (chalcopyrite, pyrite, bornite, millerite and pentlandite) and their very small grain-size (typically, <50 μm across) are characteristic features of the deposit. The *BMS* are typically enclosed by hydrous silicates (predominantly, Ca-amphibole), but some are also present as inclusions in chromite. The platinum-group minerals, *PGM* [laurite–erlichmanite, sperrylite, cooperite, hollingworthite, platarsite and isoferroplatinum (?)] are mainly present as minute (1–20 μm) inclusions in hydrous silicates and at the chromite–hydrous silicate grain boundaries. The amount of the *PGM* inclusions in chromite (predominantly, laurite–erlichmanite) is estimated to be ≤ 10–15% of the *PGM* total. Ruthenian pyrite forms a single grain (10 × 7 μm; 11.7–12.4 wt.% Ru) and a Ru-rich zone (2 × 3 μm; 6.6 wt.% Ru) within a zoned pyrite grain, which are isolated within Ca-amphibole. The malanite (3.5–4.9% Ni; 0.8–1.6% Co; 0.0–2.4% Ir; 0.4–4.3 wt.% Rh) occurs as anhedral grains (5–13 μm), enclosed within hydrous silicates. The results argue for the existence of an extensive solid-solution series between pyrite and laurite–erlichmanite, and between malanite and fletcherite. Textural data imply that the Ru-rich pyrite crystallized at a postmagmatic–hydrothermal stage, at a moderate temperature. Postcumulus re-equilibration between chromite and sulfide and enrichment of the environment in volatiles may promote the formation of the Ru-rich pyrite.

Keywords: ruthenium, platinum-group elements, platinum-group minerals, base-metal sulfides, thiospinels, ruthenian pyrite, malanite, chromitite layer, layered intrusion, Imandra complex, Russia.

Sommaire

Nous signalons la présence de pyrite ruthénienne et de malanite nickelifère anomalement appauvrie en Ir et Rh, provenant de niveaux de chromitite de la zone inférieure du complexe stratiforme d'Imandra, d'âge protérozoïque précoce, dans le secteur nord-ouest de la Russie. La très faible proportion de sulfures de métaux de base (SMB), c'est-à-dire, chalcopyrite, pyrite, bornite, millerite et pentlandite, et leur granulométrie très fine (en général, inférieure à 50 μm), sont caractéristiques du gisement. Les SMB sont typiquement inclus dans des silicates hydroxylés, surtout une amphibole calcique, mais ils peuvent aussi être inclus dans la chromite. Les minéraux du groupe du platine, laurite–erlichmanite, sperrylite, cooperite, hollingworthite, platarsite et isoferroplatinum(?), se présentent surtout en micro-inclusions (de 1 à 20 μm de taille) dans les silicates hydroxylés ou le long des contacts entre ceux-ci et la chromite. La proportion de minéraux du groupe du platine dans la chromite (laurite–erlichmanite, surtout) serait d'environ 10 à 15% du total. Un seul grain de pyrite ruthénienne a été découvert (10 × 7 μm, 11.7–12.4% Ru, par poids). De plus, un grain zoné de pyrite inclus dans l'amphibole calcique contient une zone riche en Ru (2 × 3 μm, 6.6% Ru). La malanite (3.5–4.9% Ni, 0.8–1.6% Co, 0–2.4% Ir, 0.4–4.3% Rh) se présente en grains xénomorphes (5–13 μm) inclus dans les silicates hydroxylés. Ces compositions semblent indiquer l'existence d'une solution solide étendue entre pyrite et laurite–erlichmanite, et entre malanite et fletcherite. D'après les textures, la pyrite ruthénienne aurait cristallisé à un stade post-magmatique – hydrothermal, à température modérée. Un rééquilibrage post-cumulus impliquant chromite et sulfures, et un enrichissement du milieu en phase volatile, pourraient favoriser la formation de la pyrite enrichie en Ru.

(Traduit par la Rédaction)

Mots-clés: ruthenium, éléments du groupe du platine, minéraux du groupe du platine, sulfures des métaux de base, thiospinelle, pyrite ruthénienne, malanite, niveau de chromitite, complexe intrusif stratiforme, complexe d'Imandra, Russie.

[1] *E-mail address*: barkov@sveka.oulu.fi

Introduction

The platinum-group elements (*PGE*) are well known to occur mostly as discrete minerals. To date, there are approximately one hundred platinum-group minerals (*PGM*) accepted as valid mineral species, and a large number of incompletely characterized *PGE*-bearing phases. A list of the most common *PGM* in various deposits has recently been presented by Cabri (1994). In addition, the *PGE* may occur in the form of solid solution in the major base-metal sulfides (*BMS*) and some telluride, arsenide and sulfarsenide minerals and alloys (*e.g.*, Cabri 1992). From both economic and scientific points of view, it is of great importance to know the concentration and distribution of the *PGE* and other precious elements in the essential and accessory *BMS*. However, the precious metals are typically present in trace quantities in the *BMS*, and precise techniques have to be used to detect and measure their concentrations at very low levels (*e.g.*, Cabri *et al.* 1984, Cabri *et al.* 1985, Ripley & Chryssoulis 1994, Wilson *et al.* 1995, Cabri & McMahon 1995). At the same time, pentlandite from some occurrences was reported to contain very high concentrations of the *PGE* (Genkin *et al.* 1974, Cabri *et al.* 1981, Kinloch 1982, Todd *et al.* 1982, Cabri *et al.* 1984, Tarkian & Prichard 1987, Augé 1988; J.H.G. Laflamme, unpubl. data cited in Cabri 1992).

Here, we describe the occurrence and chemistry of a Ru-rich pyrite (up to 12.4 wt.% Ru) from the Early Proterozoic Imandra (or Imandrovsky) layered complex, northwestern Russia. Typically, pyrite displays very low (ppb) levels of the *PGE* (*e.g.*, Wilson *et al.* 1995), and we are not aware of any published compositional data having been reported for *PGE*-rich pyrite from other occurrences. In recent comprehensive reviews, Cabri (1992, 1994) also did not report the presence of elevated *PGE* contents in pyrite.

Another notable feature of the occurrence reported here is the presence of a Rh–Ir-poor malanite (ideally $CuPt_2S_4$) that contains significant concentrations of nickel (up to 4.9 wt.%). Related *PGE* thiospinels from other occurrences (Yu *et al.* 1974, Cabri *et al.* 1981, Rudashevsky *et al.* 1985, Augé 1988, Corrivaux & Laflamme 1990, Ferrario & Garuti 1990, Hagen *et al.* 1990, Johan *et al.* 1990, Legendre & Augé 1992, Weiser & Schmidt-Thomé 1993, Halkoaho 1993, Augé & Maurizot 1995, Garuti *et al.* 1995) show relatively high contents of rhodium or iridium (or both).

Occurrence and Associated Minerals

A number of mafic-ultramafic intrusions and their fragments (*e.g.*, Mt. Bolshaya Varaka, Umbarechensky, Mt. Devichya, *etc.*) occur in the Lake Imandra area (Kola Peninsula), at the western and southwestern margins of the Imandra–Varzuga Supergroup of Proterozoic supracrustal rocks (Fig. 1). The size of these intrusive bodies varies from a few to several tens of km in length. According to the interpretation of Dokuchaeva *et al.* (1982, 1985), the bodies represent fragments of a single, originally very large (*ca.* 1500 km^2), layered lopolith that was broken up by intense tectonic movements. This interpretation is based on similar geological structures and compositions of the rocks and rock-forming minerals, as well as comparable element-distribution patterns observed in the different bodies. It seems, however, that more data, including isotopic compositions, are required to test the interpretation. Results of U–Pb dating (zircon) yielded an Early Proterozoic age for the Imandra complex: 2395 ± 30 Ma (Balashov *et al.* 1990) and 2441 ± 1.6 Ma (Amelin *et al.* 1995). This is in good agreement with geochronological data reported for comparable layered intrusions of the Fennoscandian Shield (Alapieti *et al.* 1990; Barkov *et al.* 1991a).

The layered series of the proposed Imandra lopolith has been divided by Dokuchaeva and coworkers into four zones: 1) A Lower Zone (*ca.* 0.15 km in thickness) composed of alternating layers of plagioclase-bearing pyroxenite, gabbronorite and norite, 2) the Main Zone (*ca.* 2 km in thickness), consisting of rather homogeneous mesocratic gabbronorite with subordinate melanocratic and leucocratic gabbronorite layers, 3) the Upper Zone (*ca.* 0.3 km), consisting of various layers of leucocratic gabbro and anorthosite, with the thickest layer of anorthosite (*ca.* 30 m) located at the uppermost stratigraphic position, 4) the Uppermost Zone (*ca.* 0.5 km) of quartz-bearing gabbro and gabbro-diorite. The total thickness of the intrusion in the exposed area reaches *ca.* 3 km. No olivine-rich cumulates were observed in the complex. The most noteworthy characteristic of the complex is the presence of chromitite layers at the lower structural levels (Kozlov *et al.* 1975, Dokuchaeva *et al.* 1985) and a diverse *PGE* mineralization closely associated with chromitite (Barkov *et al.* 1991b, 1992, 1995a, 1995b).

Both ruthenian pyrite and nickeloan malanite occur in a chromitite layer at the Mt. Bolshaya Varaka deposit. The chromitite consists of chromite (*ca.* 50 modal %) associated with hydrous silicates, mostly calcic amphibole. Typically, no relics of primary pyroxenes are preserved, but relict primary plagioclase ($An_{52.6–60.4}Ab_{39.6–47.2}Or_{0–0.2}$) is present. The hydrous minerals are characteristically rich in chromium; as much as 0.6–1.6 wt.% Cr_2O_3 was detected in calcic amphibole, and 0.9 wt.% in phlogopite. Intercumulus apatite from the chromitite typically contains chlorine (1–2 wt.%). Apatite richer in chlorine (3.6 wt.% Cl and 1.8 wt.% F) was encountered in a plagioclase-bearing pyroxenite from the same deposit. A grain of loveringite, a very rare member of the crichtonite group, was identified in spatial association with this Cl-rich apatite. The presence of end-member chlorapatite, occurring relatively near a chromitite layer, was reported by Barkov *et al.* (1995b) from the Umbarechensky intrusion, Imandra complex. In Bolshaya Varaka, we observed other Cl-rich minerals near the chromitite layer, *i.e.*, scapolite (2.2 wt.% Cl) replacing primary plagioclase, and ferroan pargasitic hornblende with 0.9 wt.% Cl. This implies that Cl was an abundant volatile phase during the post-cumulus stage of formation of the chromitite layers.

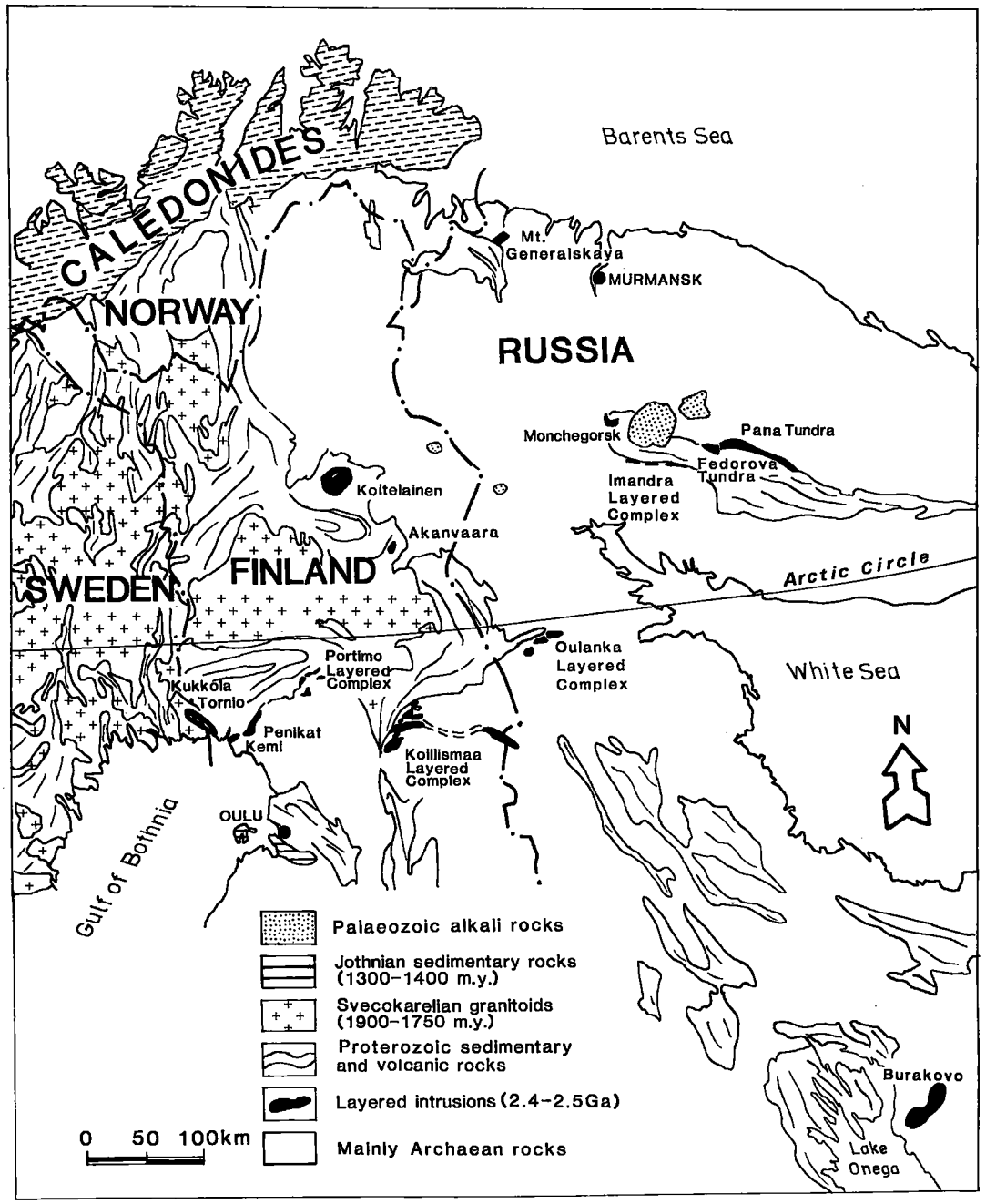

FIG. 1. A generalized geological map of part of the Fennoscandian Shield showing location of the Imandra layered complex and other Proterozoic layered intrusions. Modified from Alapieti *et al.* (1990).

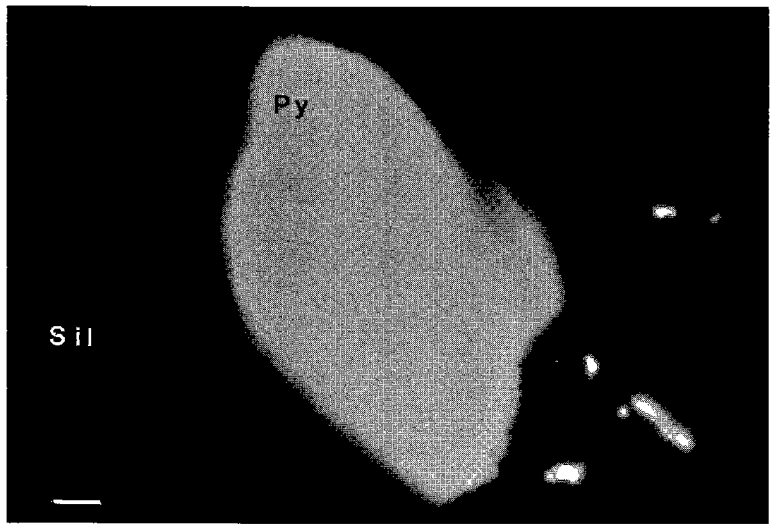

FIG. 2. A single grain of ruthenian pyrite (Py) enclosed within Ca-amphibole (Sil). Minute grains (white) within amphibole, adjacent to the ruthenian pyrite, are unidentified Rh–Ru-bearing *PGM*. Back-scattered electron image. Scale bar: 1 μm.

The *BMS* are commonly enclosed within the hydrous silicate minerals in the Bolshaya Varaka chromitite, but some grains are isolated within chromite. The very low amount of the *BMS* and their fine grain-size (typically ≤50 μm across) are particularly notable. The *BMS* are principally chalcopyrite, pyrite, bornite and millerite; pentlandite is very rare. Galena was also observed as a rare accessory phase. Identification of the *BMS* was based on both careful optical observations and electron-microprobe analyses. Some *BMS* show a euhedral habit, but the presence of euhedral bornite is most uncommon; this mineral typically occurs as anhedral grains in other occurrences. No pyrrhotite was found in Bolshaya Varaka, but it was observed in the Umbarechensky chromite deposit, along with cobaltite–gersdorffite.

The *PGM* identified in Bolshaya Varaka are predominantly members of the laurite–erlichmanite series, which are mostly located within the hydrous silicates and at chromite–silicate grain boundaries. In addition, laurite forms inclusions in chromite, but does not exceed 15% of the total amount of the *PGM* grains. It is remarkable that the members of the laurite–erlichmanite series are the only *PGM* inclusions in chromite, apart from a Pt–Fe alloy intergrown with laurite within a chromite grain. In accordance with the existing nomenclature (Cabri & Feather 1975), X-ray-diffraction data are required to classify this alloy (*i.e.*, isoferroplatinum *versus* native platinum). Unfortunately, X-ray-diffraction data could not be obtained owing to the very small size of the grain (<10 μm). However, the stoichiometric composition $(Pt_{2.85}Rh_{0.12})_{\Sigma 2.97}Fe_{1.03}$ strongly suggests that this is isoferroplatinum. Other *PGM* found are sperrylite, platarsite, hollingworthite, cooperite and Pd-bearing gold. Some compositional data on the *PGM* were presented by Barkov *et al.* (1995b).

RUTHENIAN PYRITE AND PT-RICH NICKELOAN MALANITE

The ruthenian pyrite occurs both as a single grain (10 × 7 μm; Fig. 2) and a Ru-rich zone (2 × 3 μm) within a zoned pyrite grain (*ca.* 15 μm across; Fig. 3). Both grains are hosted by calcic amphibole. The pyrite grain in Figure 3 is intergrown with chalcopyrite that is replaced by a very fine mixture of a Fe–Cu hydroxide with a hydrous silicate (?) along the periphery. A spectrum obtained in the most homogeneous area of the hydroxide shows a small chlorine peak, and a quantitative energy-dispersion (EDS) analysis gave *ca.* 0.4 wt.% Cl.

The malanite typically appears as small rounded (5–8 μm) or elongate grains (up to 13 μm in length) isolated in hydrous silicates. Both individual grains and an intergrowth with erlichmanite were observed. A cluster-like pattern of distribution of malanite and associated *PGM* (Fig. 4) occurs in a hydrous silicate.

Before carrying out the electron-microprobe analyses, the grains were carefully examined under reflected light and with scanning electron microscopy. All grains analyzed were observed to be quite homogeneous. No exsolution phases were recorded in the Ru-rich pyrite grains.

Electron-microprobe analyses (Tables 1, 2) were carried out at the Institute of Electron Optics, University of Oulu, Finland, using a JEOL JSM–6400 scanning electron microscope equipped with a LINK eXL energy-dispersion spectrometer. The analyses were performed at 15 kV and

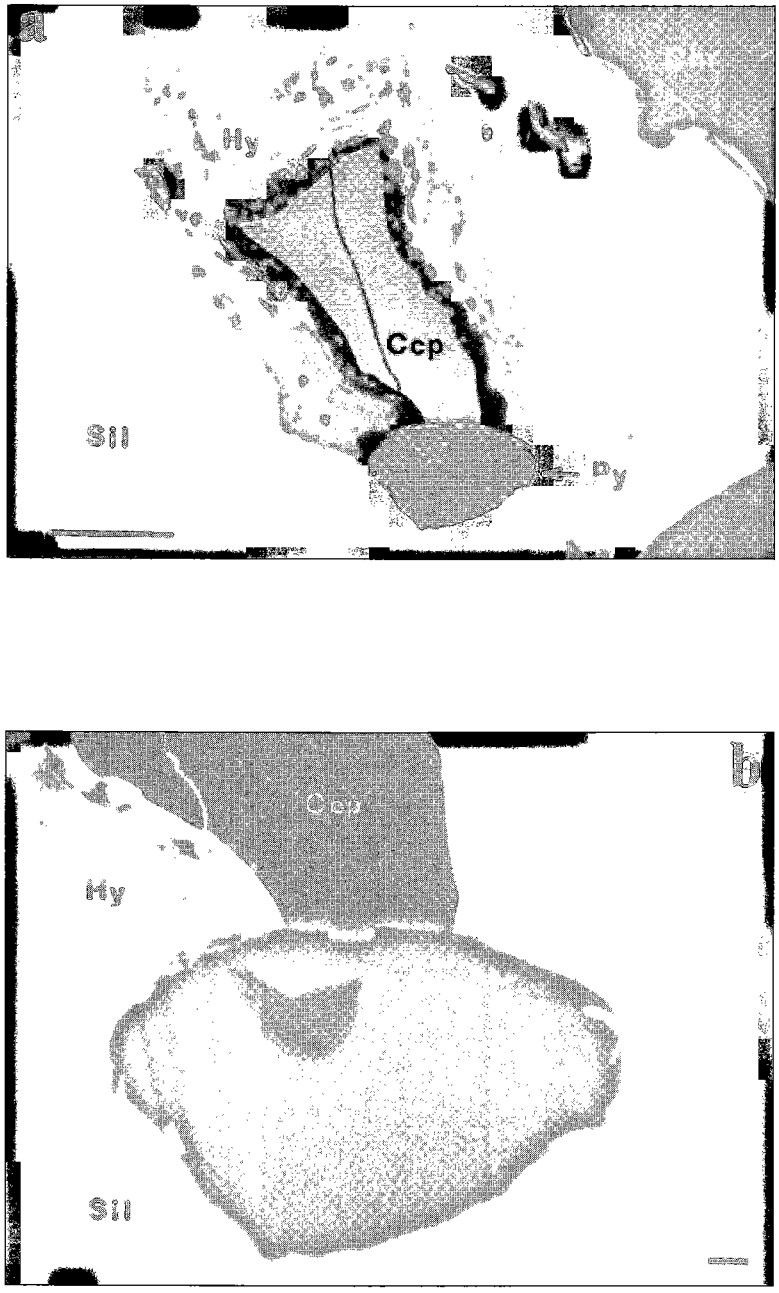

FIG. 3. (a) Zoned pyrite (Py), containing zone of ruthenian pyrite (white), intergrown with chalcopyrite (Ccp). The latter is replaced by a fine mixture of Fe–Cu hydroxide (Hy) and hydrous silicate (?). Sil = host hydrous silicate (calcic amphibole); Chr: chromite. (b) Magnification of zoned pyrite grain in Figure 3a. Note the zone of ruthenian pyrite (light) within pyrite. Abbreviations are the same as in Figure 3a. Back-scattered electron images; scale bar: 10 μm in a, 1 μm in b.

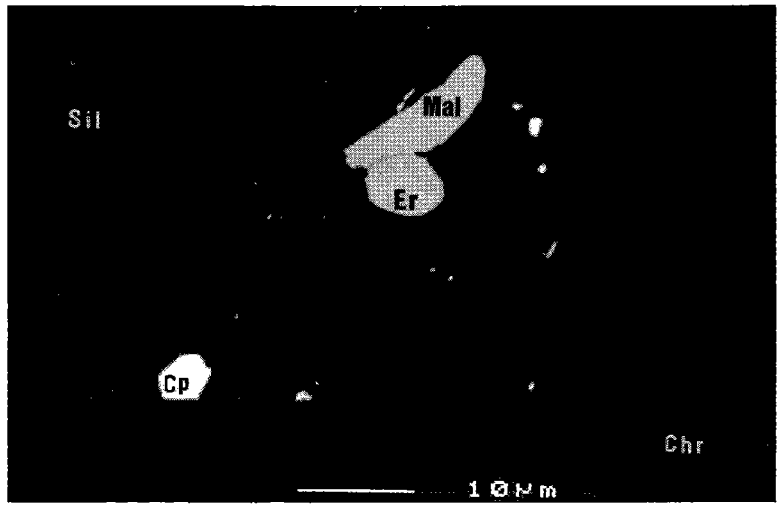

FIG. 4. A scanning electron micrograph showing malanite (Mal), erlichmanite–laurite (Er) and cooperite (Cp) grains hosted by hydrous silicate (Sil). Note minute, cluster-like *PGM* grains adjacent to the malanite-erlichmanite intergrowth. Chr: chromite. Scale bar: 10 µm.

1.2 nA, with 100-second count times. The following lines (and standards) were used: Rh*Lα* (synthetic RhSb), Pt*Mα* (PtSn), Ru*Lα*, Ir*Mα*, Cu*Kα*, Ni*Kα*, Fe*Kα*, Co*Kα* (pure elements) and S*Kα* (pyrite). Owing to the small grain-size, the most finely focused beam was used in all the analyses. The results were processed by the ZAF–4 on-line program.

Five analyses of the single grain of ruthenian pyrite, performed in different parts of the grain, yield approximately the same Ru content, *ca.* 12 wt.% (Table 1). The Ru-rich zone of the zoned grain shows significantly lower concentration of Ru (6.6 wt.%). Representative compositions of the Ru-rich pyrite are plotted in Figure 5, in comparison with compositions of *PGE*-rich pentlandite. It is important to note that some of the latter compositions may actually

TABLE 1. CHEMICAL COMPOSITION§ OF RUTHENIAN PYRITE FROM THE IMANDRA COMPLEX

	1	2	3	4	5	6
Wt.%						
Fe	36.13	36.88	37.22	36.25	37.26	41.54
Ru	12.41	11.83	11.70	12.34	12.27	6.56
S	50.54	51.24	51.61	50.62	51.10	51.75
Total	99.08	99.95	100.53	99.21	100.63	99.85
Atom.%						
Fe	27.58	27.80	27.87	27.62	28.01	30.70
Ru	5.23	4.93	4.84	5.20	5.10	2.68
S	67.19	67.27	67.29	67.18	66.90	66.62
Formula*						
Fe	0.83	0.83	0.84	0.83	0.84	0.92
Ru	0.16	0.15	0.15	0.16	0.15	0.08
ΣMet	0.99	0.98	0.99	0.99	0.99	1.00
S	2.02	2.02	2.02	2.02	2.01	2.00

§ Results of electron-microprobe analyses. 1–5: compositions determined in a single grain (*ca.* 10 × 7 µm); 6: Ru-rich zone (*ca.* 2 × 3 µm) of zoned grain (*ca.* 15 µm across). * Formula calculated on the basis of Σ atoms = 3.

TABLE 2. CHEMICAL COMPOSITION§ OF MALANITE FROM THE IMANDRA COMPLEX

		1	2	3	4*	5	6	7
Pt		55.69	56.27	56.64	55.5	49.87	50.52	50.41
Rh		nd**	nd**	nd**	0.5	4.11	4.05	4.28
Ir		nd**	nd**	nd**	nd	2.00	2.43	2.18
Cu		12.34	12.07	12.14	12.4	11.41	12.29	12.03
Ni		4.64	4.86	4.91	4.8	3.63	3.60	3.47
Co		0.95	0.80	0.80	na	1.50	1.37	1.63
Fe		0.91	0.59	0.50	0.7	0.99	1.00	1.03
S		25.32	24.36	24.49	25.4	25.39	25.71	25.65
Total		99.85	98.95	99.48	99.3	98.90	100.97	100.68
		Atomic proportions (Σ atoms = 7)						
1	Cu	0.98	0.99	0.99	1.00	0.91	0.96	0.94
2	Fe	0.02	0.01	0.01	-	0.09	0.04	0.06
3	Σ(1,2)	1.00	1.00	1.00	1.00	1.00	1.00	1.00
4	Pt	1.45	1.50	1.50	1.45	1.29	1.29	1.29
5	Rh	-	-	-	0.02	0.20	0.20	0.21
6	Ir	-	-	-	-	0.05	0.06	0.06
7	Ni	0.40	0.43	0.43	0.42	0.31	0.30	0.29
8	Co	0.08	0.07	0.07	-	0.13	0.12	0.14
9	Fe	0.06	0.05	0.04	0.06	-	0.05	0.03
10	Σ(4-9)	1.99	2.05	2.04	1.95	1.98	2.02	2.02
11	Σ Met	2.99	3.05	3.04	2.95	2.98	3.02	3.02
12	S	4.00	3.95	3.96	4.04	4.01	3.98	3.98

§ Results of electron-microprobe analyses. * Barkov *et al.* (1995b); nd: not detected, na: not analyzed. ** nd: not determined by EDS analysis (elements with counting statistics < 3 × standard deviation); WDS analysis of this malanite gave: 0–0.2 wt.% Ir (*i.e.*, ≤0.005 atoms per formula unit; Σ atoms = 7) and 0.4–0.5 wt.% Rh (*i.e.*, ~0.02 atoms per formula unit).

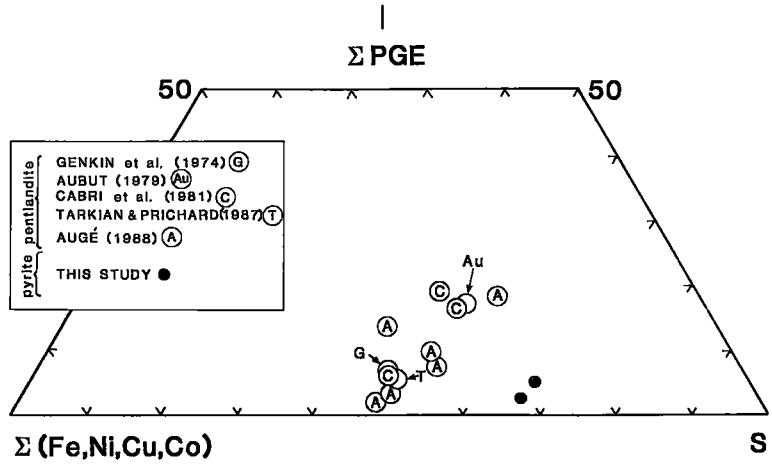

FIG. 5. Σ(Fe,Ni,Cu,Co) – Σ*PGE* – S plot of representative compositions of ruthenian pyrite (single grain and Ru-rich zone) from Imandra, compared with compositions of *PGE*-rich pentlandite from the literature.

refer to an unnamed sulfide mineral with a metals:sulfur ratio of 1:1, but not pentlandite. In view of the Ru-rich composition and the virtual absence of other *PGE*, the Ru-rich Imandra pyrite may be compared with a ruthenian pentlandite from the Shetland ophiolite (Tarkian & Prichard 1987).

Results of electron-microprobe analyses of malanite from the Imandra suite are listed in Table 2. All the compositions are consistent with the general stoichiometry of the thiospinel *PGM*: M_3S_4. Iridium and rhodium, which show counting statistics less than three times the standard deviation, were not determined in the EDS analysis of a malanite grain (anal. 1–3, Table 2). This grain (*ca.* 13 μm in length) was also analyzed using wavelength-dispersion (WDS) techniques. The WDS analyses were carried out with a Cameca Camebax electron microprobe at the University of Hamburg (courtesy of M. Tarkian), at 20 kV and 22.5 nA, using pure elements, pyrite and covellite as standards; the results were processed with a PAP program. Four WDS analyses gave 0–0.2 wt.% Ir (*i.e.*, ≤0.005 atoms per formula unit, *apfu*; Σ atoms = 7) and 0.4–0.5 wt.% Rh (*ca.* 0.02 *apfu*).

Two compositional pecularities of the Imandra thiospinels are emphasized. (1) They are Pt-rich and exceedingly poor in Ir and Rh. The members of the cupro-iridsite – cuprorhodsite – malanite group were previously known to cover a large area in the $CuIr_2S_4$–$CuRh_2S_4$–$CuPt_2S_4$ compositional space (Fig. 6), but Pt-rich phases close to pure malanite were not reported [*e.g.*, Garuti *et al.* (1995) and references therein]. The most Pt-rich compositions have recently been reported by Augé & Maurizot (1995, Fig. 13; see Fig. 6 of this paper). (2) They show a relative enrichment in Ni (up to 4.9 wt.%) and substantial Co content (1.6 wt.%). Typically, the *PGE* thiospinels from other localities show less than 1 wt.% Ni. However, Augé & Maurizot (1995) reported as much as 7.9 wt.% Ni in a highly unusual thiospinel (?) mineral from the New Caledonia ophiolite complex. The phase gives a base metals : *PGE* ratio of *ca.* 2:1 (*cf.* 1:2 in normal *PGE* thiospinels), and its composition can be recalculated to the formula $(Fe,Ni,Cu)_2(Rh,Ir)S_4$.

DISCUSSION

The results presented in this paper indicate that, similar to the *PGE*-rich pentlandite reported from a number of occurrences (Genkin *et al.* 1974, Aubut 1979, Cabri *et al.* 1981, Tarkian & Prichard 1987, Augé 1988, J.H.G. Laflamme, unpubl. data, cited in Cabri 1992), pyrite may also be a very important carrier of *PGE*. The *PGE* are widely assumed to occur in solid solution in the pentlandite, and this suggestion appears also to be valid for the Imandra ruthenian pyrite. However, most modern microbeam analytical methods, except for the SIMS technique, for instance, would not resolve so-called *invisible* precious-metal mineral grains less than 0.1 μm in diameter, colloidal-size particulates or clusters, which remain possible alternatives to true solid-solutions (Cabri 1992).

Owing to the similar ionic radii of Fe^{2+} (0.69 Å) and Ru^{4+} (0.70 Å), considered for the same coordination number (Whittaker & Muntus 1970), substitution of Ru for Fe could be significant. The following simple heterovalent substitution $2Fe^{2+} = Ru^{4+}$ is thus proposed to occur in the ruthenian pyrite. The other important factor is that pyrite is isostructural with the cubic Ru–Os disulfides laurite and erlichmanite (RuS_2 and OsS_2, respectively), which belong to the pyrite structural group (*Pa*3). A complete solid-solution series exists between laurite and erlichmanite

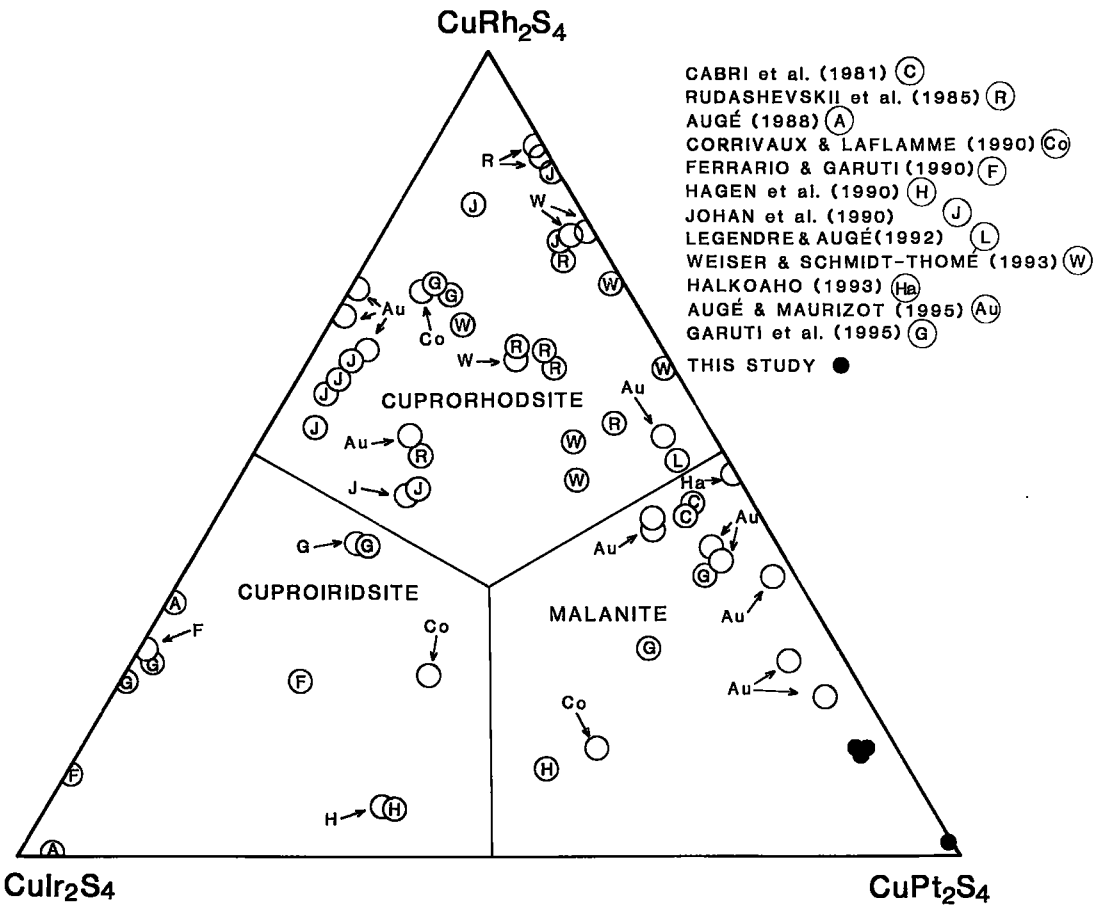

FIG. 6. Ir–Rh–Pt plot of representative compositions of malanite from Imandra, compared with data from the literature.

(*e.g.*, Bowles *et al.* 1983), the cell sizes of which are very close to each other: a between 5.59 and 5.61 Å for laurite and a = 5.62 Å for erlichmanite (Leonard *et al.* 1969, Snetsinger 1971, Bowles *et al.* 1983). Therefore, the existence of an extensive solid-solution series between pyrite (a = 5.42 Å; Ramdohr 1980) and laurite–erlichmanite is plausible. By analogy with *PGE*-rich pentlandite, pyrite containing *PGE* other than Ru can also be expected to occur in nature.

Obviously, particular conditions are required for crystallization of the *PGE*-rich pyrite, as well as the other *PGE*-bearing *BMS*. The fact that these minerals typically occur in close association with chromite (*e.g.*, Genkin 1974, Tarkian & Prichard 1987, Augé 1988) may be of genetic importance. The very low sulfide content, very small grain-size of the *BMS*, and the Cu-rich character of the *BMS* mineralization in Imandra, are consistent with subsolidus re-equilibration (Von Gruenewaldt *et al.* 1986) or high-temperature reaction (Naldrett & Von Gruenewaldt 1989) between chromite and sulfide during cooling. Under such conditions, the removal of Fe from the sulfide may have caused a local deficiency of iron and a considerable increase in the relative amount of the *PGE* in the remaining sulfide, favoring incorporation of ruthenium instead of iron in the structure of the growing pyrite.

The Imandra Ru-rich pyrite is thought to have formed under conditions of elevated activity of fluid, which are confirmed by the presence of abundant volatile-bearing minerals in the chromitite layer and in its vicinity. Furthermore, this pyrite was only found to be hosted by hydrous silicates. Regarding the Merensky Reef, Kinloch & Peyerl (1990) postulated that a strong enrichment in volatiles may have resulted in the lowering of crystallization temperatures and delayed crystallization of high-temperature *PGM*. Consequently, more *PGE* remained in solid solution in the *BMS*. Cabri (1992) mentioned that compositional data for pentlandite in potholes and the normal reef seem to be in agreement with this suggestion.

In case of the Imandra chromitite, a fluid-rich environment may have caused, at least locally, a delayed

crystallization of laurite. The liquidus temperature was lowered and, hence, there was not sufficient time for crystallization of the laurite. At a relatively low temperature, when laurite could not crystallize, but at a stage when ruthenium was already present, the ruthenian pyrite formed. An alternative is that Ru was removed from the primary laurite–erlichmanite by a late fluid activity and precipitated as the ruthenian pyrite.

Owing to a lack of experimental data, the temperature of formation of the ruthenian pyrite is not rigorously constrained. At low pressures, normal pyrite is stable up to 743°C (*e.g.*, Kullerud & Yoder 1959, Deer *et al.* 1962). The characteristic intergrowths of chalcopyrite and pyrite at Imandra suggest their formation at a temperature of less than 739°C, since these *BMS* cannot exist together above this temperature. No intergrowth relationships between pyrite and bornite were observed in the occurrence, but the close spatial association of these minerals in the chromitite strongly suggests a maximum temperature of 568°C at which this assemblage may exist in the system Cu–Fe–S (Deer *et al.* 1962). However, the high Ru content should increase to some extent the temperature of formation of ruthenian pyrite, compared with that of normal pyrite and its synthetic equivalent. Nevertheless, the textural data strongly suggest that the Ru-rich pyrite formed at a post-magmatic – hydrothermal stage, and imply a moderate temperature for its crystallization.

This study establishes the occurrence of Pt-rich and Ir–Rh-poor nickeloan malanite and confirms continuous solid-solution in the system $CuRh_2S_4$–$CuIr_2S_4$–$CuPt_2S_4$. The Imandra malanite is unusual among the other *PGE* thiospinel minerals, in that it displays a Ni-for-*PGE* (Pt) type of substitution. This is confirmed by the empirical formulae (anal. 1–4, Table 2), the copper content of which is very close to 1 (0.98–1.00) *apfu*, whereas the Σ(Pt,Ni,Co,Fe) is very close to 2 *apfu*. The existence of a solid-solution series between malanite and (Cu)–Ni–Co thiospinels (fletcherite and carrollite: ideally $CuNi_2S_4$ and $CuCo_2S_4$, respectively) is clearly suggested by the data and strongly supported by similarities in the unit-cell parameters of the thiospinel minerals. Malanite was previously proposed to be cubic with a = 6.03 Å (Yu *et al.* 1974), but Rudashevsky *et al.* (1984) proved that its cell size is 9.94 Å, in common with those of cuprorhodsite (a = 9.88 Å) and cupro-iridsite (a = 9.92 Å). The a cell sizes of fletcherite and carrollite are 9.520 and 9.477 Å, respectively (Craig & Carpenter 1977). All these thiospinels crystallize in space group *Fd3m*. Therefore, the structural similarities favor the existence of wide ranges of solid solution between the *PGE*-bearing and (Cu)–Ni–Co thiospinels.

Acknowledgements

This paper is a contribution from the Research project "Ore Processes and Geotectonics" (University of Oulu) funded by the Academy of Finland. A.Y.B. thanks the Centre for International Mobility, Finland, and the University of Oulu for research grants. We thank Dr. L.J. Cabri for providing the PGE microprobe standards used in this research, and Prof. M. Tarkian and B. Cornelisen for providing the WDS electron-microprobe analyses. The comments and suggestions of two referees, Prof. M.E. Fleet and Dr. P. Hofmeyr, and Associate Editor, Dr. S.L. Chryssoulis, on an earlier version of this manuscript are greatly appreciated, as is the editorial assistance of R.F. Martin and W.H. MacLean. We also thank K. Karjalainen for drafting the figures.

References

Alapieti, T.T., Filén, B.A., Lahtinen, J.J., Lavrov, M.M., Smolkin, V.F. & Voitsekhovsky, S.N. (1990): Early Proterozoic layered intrusions in the northeastern part of the Fennoscandian Shield. *Mineral. Petrol.* **42**, 1-22.

Amelin, Y.V., Heaman, L.M. & Semenov, V.S. (1995): U–Pb geochronology of layered mafic intrusions in the eastern Baltic Shield: implications for the timing and duration of Paleoproterozoic continental rifting. *Precambrian Res.* **75**, 31-46.

Aubut, A.J. (1979): *The Geology and Mineralogy of a Tertiary Buried Placer Deposit, Southern British Columbia.* M.Sc. thesis, Univ. of Alberta, Edmonton, Alberta.

Augé, T. (1988): Platinum-group minerals in the Tiebaghi and Vourinos ophiolitic complexes: genetic implications. *Can. Mineral.* **26**, 177-192.

_____ & Maurizot, P. (1995): Stratiform and alluvial platinum mineralization in the New Caledonia ophiolite complex. *Can. Mineral.* **33**, 1023-1045.

Balashov, Y.A., Amelin, Y.V., Bayanova, T.B., Gannibal, L.F., Zhangurov, A.A., Koshcheev, O.A., Ryungenen, G.I., Fedotov, Zh.A., Sharkov, I.V. & Sherstennikova, O.G. (1990): The Imandra lopolith. *In* New Data on Geochronology and Isotope Geochemistry of Precambrian Rocks of the Kola Peninsula **1**. Kola Science Centre, Apatity, Russia (14-20; in Russian).

Barkov, A.Y., Gannibal, L.F., Ryungenen, G.I. & Balashov, Y.A. (1991a): A U–Pb dating of zircons from the Kivakka layered intrusion, northern Karelia. *In* All-Union Conf. on Methods of Isotope Geology (St. Petersburg), 21-23 (in Russian).

_____, Lednev, A.I., Trofimov, N.N. & Lavrov, M.M. (1991b): Minerals of the laurite–erlichmanite series from chromitite layers of layered intrusions in the Karelia–Kola region. *Dokl. Akad. Nauk* **319**, 962-965 (in Russian).

_____, _____ & Zhangurov, A.A. (1992): PGE-mineralization in a chromitite layer of the Imandrovsky layered intrusion, Kola Peninsula. *In* Geology and Genesis of the Platinum-Metal Deposits, Proc. Conf. (Moscow), 101 (in Russian).

_____, Pakhomovskii, Ya.A. & Men'shikov, Y.P. (1995a): Zoning in the platinum-group sulfide minerals from the Lukkulaisvaara and Imandrovsky layered intrusions, Russia. *Neues Jahrb. Mineral., Abh.* **169**, 97-117.

_____, SAVCHENKO, YE.E. & ZHANGUROV, A.A. (1995b): Fluid migration and its role in the formation of platinum-group minerals: evidence from the Imandrovsky and Lukkulaisvaara layered intrusions, Russia. *Mineral. Petrol.* **54**, 249-260.

BOWLES, J.F.W., ATKIN, D., LAMBERT, J.L.M., DEANS, T. & PHILLIPS, R. (1983): The chemistry, reflectance, and cell size of the erlichmanite (OsS_2) – laurite (RuS_2) series. *Mineral. Mag.* **47**, 465-471.

CABRI, L.J. (1992): The distribution of trace precious metals in minerals and mineral products. *Mineral. Mag.* **56**, 289-308.

_____ (1994): Current status of determination of mineralogical balances for platinum-group element-bearing ores. *Trans. Inst. Mining Metall., Sect. B: Appl. Earth Sci.* **103**, B3-B9.

_____, BLANK, H., EL GORESY, A., LAFLAMME, J.H.G., NOBILING, R., SIZGORIC, M.B. & TRAXEL, K. (1984): Quantitative trace-element analyses of sulfides from Sudbury and Stillwater by proton microprobe. *Can. Mineral.* **22**, 521-542.

_____, CAMPBELL, J.L., LAFLAMME, J.H.G., LEIGH, R.G., MAXWELL, J.A. & SCOTT, J.D. (1985): Proton-microprobe analysis of trace elements in sulfides from some massive-sulfide deposits. *Can. Mineral.* **23**, 133-148.

_____, CRIDDLE, A.J., LAFLAMME, J.H.G., BEARNE, G.S. & HARRIS, D.C. (1981): Mineralogical study of complex Pt–Fe nuggets from Ethiopia. *Bull. Minéral.* **104**, 508-525.

_____ & FEATHER, C.E. (1975): Platinum-iron alloys: a nomenclature based on a study of natural and synthetic alloys. *Can. Mineral.* **13**, 117-126.

_____ & MCMAHON, G. (1995): SIMS analysis of sulfide minerals for Pt and Au: methodology and relative sensitivity factors (RSF). *Can. Mineral.* **33**, 349-359.

CORRIVAUX, L. & LAFLAMME, J.H.G. (1990): Minéralogie des éléments du groupe du platine dans les chromitites de l'ophiolite de Thetford Mines, Québec. *Can. Mineral.* **28**, 579-595.

CRAIG, J.R. & CARPENTER, A.B. (1977): Fletcherite, $Cu(Ni,Co)_2S_4$, a new thiospinel from the Viburnum Trend (New Lead Belt), Missouri. *Econ. Geol.* **72**, 480-486.

DEER, W.A., HOWIE, R.A. & ZUSSMAN, J. (1962): *Rock-Forming Minerals.* **5.** *Non-silicates.* Longmans, London, U.K.

DOKUCHAEVA, V.S., ZHANGUROV, A.A. & FEDOTOV, ZH.A. (1982): The Imandra lopolith – a new large layered intrusion in the Kola Peninsula. *Dokl. Akad. Nauk* **265**, 1231-1234 (in Russian).

_____, _____ & _____ (1985): Distribution patterns of chromite and titanomagnetite deposits in the Imandra intrusion (Monchegorsk district). *In* Prognosis of Ore Deposits in the Kola Peninsula. Kola Science Centre, Apatity, Russia (77-84; in Russian).

FERRARIO, A. & GARUTI, G. (1990): Platinum-group mineral inclusions in chromitites of the Finero mafic–ultramafic complex (Ivrea-Zone, Italy). *Mineral. Petrol.* **41**, 125-143.

GARUTI, G., GAZZOTTI, M. & TORRES-RUIZ, J. (1995): Iridium, rhodium, and platinum sulfides in chromitites from the ultramafic massifs of Finero, Italy, and Ojén, Spain. *Can. Mineral.* **33**, 509-520.

GENKIN, A.D., LAPUTINA, I.P. & MURAVITSKAYA, G.N. (1974): Ruthenium- and rhodium-containing pentlandite – an indicator of hydrothermal mobilization of platinum metals. *Int. Geol. Rev.* **18**, 723-728.

HAGEN, D., WEISER, T. & HTAY, T. (1990): Platinum-group minerals in Quaternary gold placers in the upper Chindwin area of northern Burma. *Mineral. Petrol.* **42**, 265-286.

HALKOAHO, T. (1993): *The Sompujärvi and Ala–Penikka PGE Reefs in the Penikat Layered Intrusion, Northern Finland: Implications for PGE Reef-Forming Processes.* Ph.D. thesis, Univ. of Oulu, Oulu, Finland.

JOHAN, Z., OHNENSTETTER, M., FISCHER, W. & AMOSSÉ, J. (1990): Platinum-group minerals from the Durance river alluvium, France. *Mineral. Petrol.* **42**, 287-306.

KINLOCH, E.D. (1982): Regional trends in the platinum-group mineralogy of the Critical Zone of the Bushveld Complex, South Africa. *Econ. Geol.* **77**, 1328-1347.

_____ & PEYERL, W. (1990): Platinum-group minerals in various rock types of the Merensky reef: genetic implications. *Econ. Geol.* **85**, 537-555.

KOZLOV, M.T., LATYSHEV, L.N., DOKUCHAEVA, V.S., BARTENEV, I.S., SHLYAKHOVA, KH.T., KOSTIN, S.M. & PAKHOMOVSKII, YA.A. (1975): A new type of chromite ore in the quartz-bearing gabbronorites of the Monchegorsk area. *In* Basic and Ultrabasic Rocks of the Kola Peninsula and their Metallogeny. Kola Science Centre, Apatity, Russia (108-125; in Russian).

KULLERUD, G. & YODER, H.S., JR. (1959): Pyrite stability relations in the Fe–S system. *Econ. Geol.* **54**, 533-572.

LEGENDRE, O. & AUGÉ, T. (1992): Alluvial platinum-group minerals from Manampotsy area, East Madagascar. *Aust. J. Earth Sci.* **39**, 389-404.

LEONARD, B.F., DESBOROUGH, G.A. & PAGE, N.J. (1969): Ore microscopy and chemical composition of some laurites. *Am. Mineral.* **54**, 1330-1346.

NALDRETT, A.J. & VON GRUENEWALDT, G. (1989): Association of platinum-group elements with chromitite in layered intrusions and ophiolite complexes. *Econ. Geol.* **84**, 180-187.

RAMDOHR, P. (1980): *The Ore Minerals and their Intergrowths.* Akademie-Verlag, Berlin, Germany.

RIPLEY, E.M. & CHRYSSOULIS, S.L. (1994): Ion microprobe analysis of platinum-group elements in sulfide and arsenide minerals from the Babbitt Cu–Ni deposit, Duluth complex, Minnesota. *Econ. Geol.* **89**, 201-210.

RUDASHEVSKY, N.S., MEN'SHIKOV, YU.P., MOCHALOV, A.G., TRUBKIN, N.V., SHUMSKAYA, N.I. & ZHDANOV, V.V. (1985): Cuprorhodsite $CuRh_2S_4$ and cuproiridsite $CuIr_2S_4$, new natural

thiospinels of the platinum-group elements. *Zap. Vses. Mineral. Obshchest.* **114**, 187-195 (in Russian).

_____, MOCHALOV, A.G., SHKURSKY, V.V., SHUMSKAYA, N.I. & MEN'SHIKOV, YU.P. (1984): The first discovery of malanite $Cu(Pt,Ir,Rh)_2S_4$ in the USSR. *Mineral. Zh.* **6**, 93-97 (in Russian).

SNETSINGER, K.G. (1971): Erlichmanite, OsS_2, a new mineral. *Am. Mineral.* **56**, 1501-1506.

TARKIAN, M. & PRICHARD, H.M. (1987): Irarsite–hollingworthite solid-solution series and other associated Ru-, Os-, Ir-, and Rh-bearing PGM's from the Shetland ophiolite complex. *Mineral. Deposita* **22**, 178-184.

TODD, S.G., KEITH, D.W., LE ROY, L.W., SCHISSEL, D.J., MANN, E.L. & IRVINE, T.N. (1982): The J–M platinum–palladium reef of the Stillwater complex, Montana. I. Stratigraphy and petrology. *Econ. Geol.* **77**, 1454-1480.

VON GRUENEWALDT, G., HATTON, C.J., MERKLE, R.K.W. & GAIN, S.B. (1986): Platinum-group element – chromite associations in the Bushveld complex. *Econ. Geol.* **81**, 1067-1079.

WEISER, T. & SCHMIDT-THOMÉ, M. (1993): Platinum-group minerals from the Santiago river, Esmeraldas province, Ecuador. *Can. Mineral.* **31**, 61-73.

WHITTAKER, E.J.W. & MUNTUS, R. (1970): Ionic radii for use in geochemistry. *Geochim. Cosmochim. Acta* **34**, 945-956.

WILSON, G.C., KILIUS, L.R. & RUCKLIDGE, J.C. (1995): Precious metal contents of sulfide, oxide and graphite crystals: determinations by accelerator mass spectrometry. *Econ. Geol.* **90**, 255-270.

YU, T.-H., LIN, S.-J., CHAO, P., FANG, C.-S. & HUANG, C.-S. (1974): A preliminary study of some new minerals of the platinum-group and another associated new one in platinum-bearing intrusion in a region in China. *Acta Geol. Sinica* **2**, 202-218 (in Chinese).

Received June 1, 1996, revised manuscript accepted March 30, 1997.